ARTICLE

BIOTECHNOLOGY and BIOENGINEERING

Growth Kinetics of Microalgae in Microfluidic Static Droplet Arrays

Alim Dewan, Jihye Kim, Rebecca H. McLean, Siva A. Vanapalli, Muhammad Nazmul Karim

Department of Chemical Engineering, Texas Tech University, Lubbock, Texas 79409; telephone: 806-742-3553; fax: 806-742-3552; e-mail: siva.vanapalli@ttu.edu; naz.karim@ttu.edu

ABSTRACT: We investigated growth kinetics of microalgae, *Chlorella vulgaris*, in immobilized arrays of nanoliter-scale microfluidic drops. These static drop arrays enabled simultaneous monitoring of growth of single as well as multiple cells encapsulated in individual droplets. To monitor the growth, individual drop volumes were kept nearly intact for more than a month by controlling the permeation of water in and out of the microfluidic device. The kinetic growth parameters were quantified by counting the increase in the number of cells in each drop over time. In addition to determining the kinetic parameters, the cell-size distribution of the microalgae was correlated with different stages of the growth. The single-cell growth kinetics of *C. vulgaris* showed significant heterogeneity. The specific growth rate ranged from 0.55 to 1.52 day^{-1} for different single cells grown in the same microfluidic device. In comparison, the specific growth rate in bulk-scale experiment was 1.12 day^{-1}. It was found that the average cell size changes significantly at different stages of the cell growth. The mean cell-size increased from 5.99 ± 1.08 to 7.33 ± 1.3 μm from exponential to stationary growth phase. In particular, when multiple cells are grown in individual drops, we find that in the stationary growth phase, the cell size increases with the age of cell suggesting enhanced accumulation of fatty acids in older cells.

Biotechnol. Bioeng. 2012;xxx: xxx–xxx.

KEYWORDS: single cell; microalgae; growth kinetics; *Chlorella vulgaris*; microfluidics; droplet arrays

Introduction

Due to growing concern over future availability, cost, environmental impact, and geopolitics of fossil fuel there is a renewed interest in third generation biofuels such as algal biodiesel (Rittmann, 2008; Rodolfi et al., 2009; Tang et al., 2011; Weyer et al., 2010). There are many algal biodiesel companies which have been formed in recent years; however, these industries are still in the research and development stage. The success of these companies hinges on finding high oil producing strains, identifying the environmental conditions for rapid growth of algae, and most importantly understanding of the basic cellular phenomena controlling algal oil content (Wu et al., 2011). Fundamental understanding of the cellular phenomena requires detailed investigations of the growth of single cells in response to chemical and biological cues such as substrate composition, temperature, light, pH, and genetic modification, and the physical cues such as flow conditions, cell size, and shear stress. The first step in investigating the single-cell phenomena is to isolate and grow individual cells in a well-defined environment. In this study, we use drop-based microfluidics to isolate single microalgae cells in nanoliter-scale droplets and monitor their growth. *Chlorella vulgaris* is chosen as the model organism because it is a well-known microalgae, which is used in various laboratories and can be grown hetero-autotropically.

Currently, several tools exist to monitor the growth of algae. The most popular ones are bioreactors which are used to observe the growth kinetics in bulk (Chen et al., 2010; Liang et al., 2009). The kinetic parameters are quantified by measuring the optical density or biomass or the cell number in representative samples collected from the bioreactor (Powell et al., 2009). The measured kinetic parameters from such approaches represent a statistical average of the properties of all the cells. Therefore bioreactor-based approaches are incapable of tracking the growth kinetics of individual cells and its progeny. Flow cytometry is another method that is used for sorting cells, determining cell size, and identifying intracelluar organells (Collier, 2000; Koch et al., 1996). However, flow cytometry

Correspondence to: M. N. Karim and S. A. Vanapalli
Contract grant sponsor: AT & T Foundation, Texas Tech University
Contract grant sponsor: Agriculture and Food Research Initiative
Contract grant number: 2009-02400
Contract grant sponsor: USDA National Institute of Food and Agriculture
Contract grant sponsor: Texas Tech University Honors College
Received 6 March 2012; Revision revised 24 April 2012; Accepted 18 May 2012
Accepted manuscript online xx Month 2012;
Article first published online in Wiley Online Library (wileyonlinelibrary.wiley.com).
DOI 10.1002/bit.24568

allows only single time-point measurements of a cell without tracking the changes in the cell and its descendents (Kortmann et al., 2009). Microwell plates are also used to monitor the growth of cells (Lindström, 2009; Onoe and Takeuchi, 2008). However, it is difficult to isolate single cells in the wellplates. Moreover, the fluid volumes in multiwell plates are prone to evaporative losses, preventing long-term cellular assays unless the plates are maintained in humid growth chambers or samples are overlaid with oil.

In contrast to the above-mentioned approaches, drop-based microfluidics is an attractive platform to investigate cellular phenomena. Microfluidic drops enable encapsulation of single to many cells in high-throughput fashion (Um et al., 2010). The growth kinetics of individual cells and their progeny can be monitored over a long period of time, particularly when the drops are immobilized. These immobilized droplets act as miniaturized batch bioreactors. In addition, since the droplets are distributed over a small area, it is easier to expose all cells to the same environmental conditions such as light and temperature. Considering these advantages, several studies have exploited microfluidic drops for analysis of single cells including bacteria (Huebner et al., 2007; Lee et al., 2006; Shim et al., 2009), mammalian (Brouzes et al., 2009), yeast (Falconnet et al., 2011; Kortmann et al., 2009; Koster et al., 2008), and algae cells (Pan et al., 2011). For example, Huebner et al. (2007) used microfluidic droplets for quantitative detection of fluorescent protein expressed in single *Escherichia coli* bacteria (Huebner et al., 2007). Marcoux et al. (2011) monitored glucoronidase enzyme activity of single-bacterial cell for over 24 h in water-in-oil emulsion droplets (Marcoux et al., 2011). Koster et al. (2008) used picoliter-scale droplets to encapsulate and grow single mouse hybridoma cells for 6 h (Koster et al., 2008).

An important consideration when immobilized drops are used for cellular analysis is the ability to keep the volume of the drop intact over long periods of time. Previously, researchers have used different approaches to store droplets for prolonged durations. Trivedi et al. (2010) used teflon tube to store the droplets. They observed cell viability inside the droplets for 9 days, although they did not report about the change of size of the droplets. Marcoux et al. (2011) used water-in-oil emulsion droplets, however, the smaller droplets coalesced with larger drops limiting the storage to 24 h. Although the use of polydimethylsiloxane (PDMS) devices is popular in drop-based microfluidics, storage of drops in such devices can be problematic due to PDMS being porous. The diffusion of water through the pores can vary the size of the droplets over time (Shim et al., 2007). Drop shrinkage in PDMS devices can be mitigated using several approaches including placing glass slides over PDMS or creating a water reservoir around the device to saturate PDMS (Schmitz et al., 2009; Pan et al., 2011). Prolonged drop storage can also be achieved using a thin PDMS membrane as the bottom layer of the device, and placing it in a water reservoir (Shim et al., 2007). This method allows the water that escapes through the top PDMS surface to be compensated by water that diffuses through the thin bottom layer.

The focus of our work is to investigate the growth kinetics of C. *vulgaris* at the level of single or few cells and relate the growth parameters to changes in cell size distribution. Our investigation on C. *vulgaris* was particularly challenging because these cells reach the stationary growth phase in 8–12 days (Liang et al., 2009), necessitating storage of microfluidic drops for at least 2 weeks without significant shrinkage of drop volumes. To achieve long-term storage of microfluidic drops, we adopted the droplet storage method reported by Shim et al. (2009, 2007) with some modifications.

In this article, we report (i) the design and fabrication of the microfluidic device for storing drops, (ii) the techniques used for immobilizing the droplets, cell encapsulation, and the long-term storage of the droplets to study growth kinetics of *C. vulgaris*, (iii) results of growth kinetics of single and few cells of *C. vulgaris*, and (iv) change of cell-size distribution at different stages of the growth. In all the microfluidic droplet experiments, the growth of the algae was quantified by counting the total cell population inside the droplets. The microfluidic experimental results were compared with the results from traditionally used bulk scale experiments.

Experimental

Microfluidic Device Design and Fabrication

Details of the microfluidic device design and fabrication have been reported in our previous work (Bithi and Vanapalli, 2010). Briefly, the device has a fluidic network and an upstream T-junction to generate drops as shown in Figure 1. The fluidic network contains a repeated sequence of loops. Each loop had two branches with the lower branch containing a hydrodynamic trap. The upper branch was a rectangular channel with uniform width (200 μm). The lower branch was divided into four sections: three rectangular sections (100 μm each) and one circular section, which was the hydrodynamic trap (385 μm). The ratio of the hydrodynamic resistances of the lower to upper branch resistance was 0.83. The device had a uniform height 80 μm.

The microfluidic devices were prepared using soft lithography. A mold was fabricated in SU-8 (2050, Microchem, Inc., Santa Clara, CA) using standard photolithography. The microfluidic device consisted of two layers of PDMS (Sylgard® 1 82 silicone elastomer base and curing agent mixed in the ratio of 10:1). The top layer contained the fluidic network and the bottom layer was plain PDMS membrane. The top layer was prepared by polymerizing the PDMS on the SU-8 mold at 60°C for 2 h. The thickness of the top layer was ~4 mm. The bottom layer was prepared by spincoating on a silanized slicon wafer disk. A certain amount of PDMS was poured on the wafer and spun at ~1,200 rpm for 30 s. The weight of the PDMS layer was

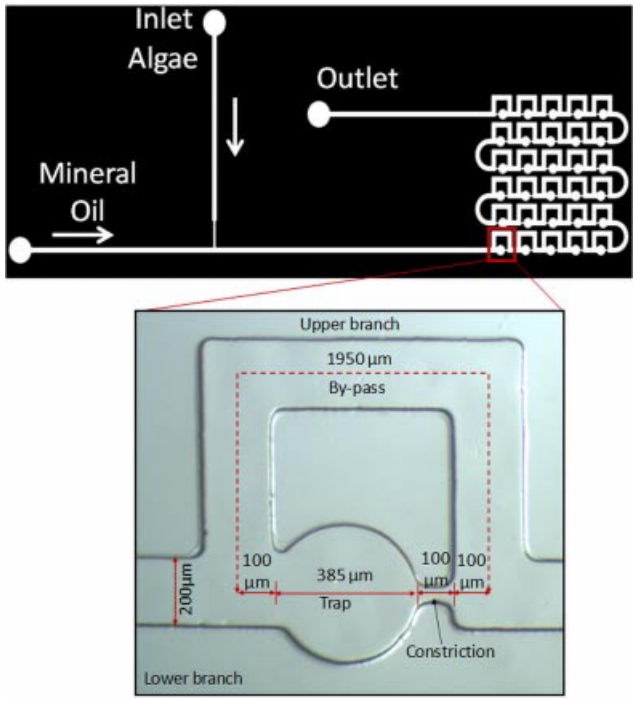

Figure 1. Schematic diagram of the PDMS microfluidic device and the magnified image of a loop highlighting the various geometric dimensions. Detail design of this device is described in Bithi and Vanapalli (2010).

monitored by weighing before and after the spinning. The thickness was calculated using the measured weight, the known density of the PDMS, and known diameter of the wafer disk. The thickness of the bottom PDMS layer typically ranged from 80 to 100 μm.

Generation of Static Droplet Arrays for Algal Culture

Our method for generating static droplet arrays builds upon the work of Boukellal et al. (2009). We used hydrostatic pressure for driving the oil and water phases into the device. The hydrostatic pressure was created by varying the vertical position of the sample vials containing the algae culture and the mineral oil. The positions of the vials were manipulated using micromanipulator attached to a wooden frame as shown in Figure 2A. The position of the vials was varied from 19 to 35 cm from the bottom of the PDMS chip. The actual height was adjusted manually by observing the position of the two-phase interface in the T-junction under the microscope.

To trap the droplets, initially, the height of the vial containing oil phase was increased and the entire channel network of the chip was filled with mineral oil. Once the entire channel network was filled with mineral oil, the algae culture was introduced up to the point shown in Figure 2B(i). Then, the height of the vial with algae culture was slowly increased to a point so that a long plug of algae culture medium entered the fluidic network at the T-junction as shown in Figure 2B(ii). While introducing the algae culture, the height of the vial with oil was positioned in such a way that the plug of the algae culture did not enter into the mineral oil inlet (Fig. 1). Once a long plug of algae culture entered the chip, the height of the mineral oil vial was increased and, at the same time, the height of the algae culture vial was decreased to new positions so that a single algae culture plug was generated as shown in Figure 2B(iii). The length of the plug was tuned depending on the number of droplets to be trapped. To trap 30 droplets, we typically needed a plug length of at least 25 mm.

In Figure 2B(v) to (x), we show the sequence of steps leading to the formation of static drop arrays from a single plug. Initially, the plug enters into the lower branch because its hydrodynamic resistance is smaller than the hydrodynamic resistance of the upper branch (Fig. 2B(v)). When the plug fills the hydrodynamic trap, the resistance of the lower branch increases and the liquid from the rest of the plug starts to move forward through the upper branch (Fig. 2B(vi)) to the next loop (Fig. 2B(vii)). When the tail of the plug passes the first loop (Fig. 2B(viii)), the first droplet is created by break-up of the long plug as shown in Figure 2B(ix). This process repeats at each of the loops, creating an array of immobilized drops (Fig. 2B(x)). Once all the droplets are created, the oil flow is continued further to flush any cells or debris in the fluidic network. Figure 2C shows the final outcome, where 30 uniformly sized droplets are arrayed in the microfluidic device. The volume of each droplet is ~10 nL.

To maintain the individual drop volumes intact for prolonged duration, the device was stored in a Petri dish filled with deionized water as shown in Figure 3. The use of thin membrane at the bottom of the chip allowed water to diffuse into the droplets to make up for the loss of water from the droplet through the top layer. The diffusion rate of water from the droplets is dependent upon the thickness of the top and bottom layer of the chip, the room temperature, and the humidity (Shim et al., 2007). If the room temperature and the humidity are kept constant, the diffusion rate can be set by changing the thickness of the top and bottom layer of the chip. To simplify the technique, instead of the changing the thickness of the PDMS layers of the chip, we varied the area of the aperture of the cover of the Petri dish to control the diffusion (Fig. 3). This also allowed us to minimize the effect of any fluctuations in the room temperature and the humidity. Moreover, the inlet and outlet reservoirs on the device were filled with mineral oil so that air could not enter into the fluidic network due to permeation-driven flow (Doyle and Randall, 2005).

The Culture of Microalgae

C. vulgaris was obtained from the University of Texas at Austin Culture Collection (UTEX, # 2714). The growth

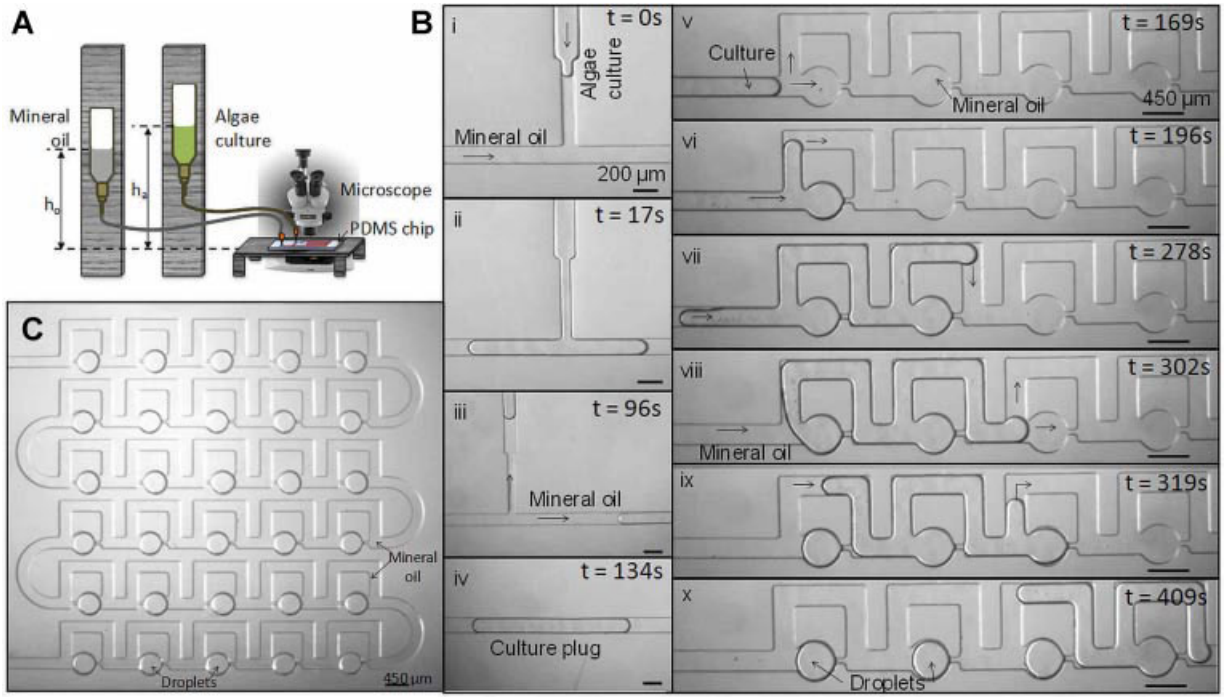

Figure 2. Droplet trapping using hydrostatic pressure. **A**: Schematic of the experimental setup of the hydrostatic pressure head for trapping the droplets, (**B**) time-stamped images showing the formation of single algae culture plug (i–iv) and droplet arrays (v–x), and (**C**) the microchip after trapping 30 droplets.

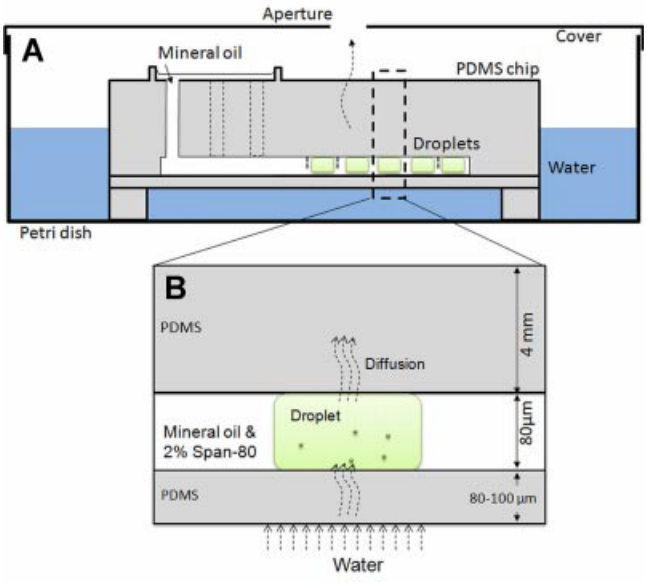

Figure 3. Long-term storage of the droplets. **A**: A schematic diagram depicting the set-up for prolonged storage of microfluidic drops, and (**B**) magnified view indicating the mechanism regulating intact storage of drops over a long duration. The broken arrows indicate permeation of water.

medium contained 10 g/L glucose, 1 g/L yeast extract mixed with proteose medium formulated by UTEX. The proteose medium contained 1 g/L proteose peptone (BD 211684), 2.94 mM $NaNO_3$ (Fisher, Waltham, MA, BP360-500), 0.17 mM $CaCl_2{\cdot}2H_2O$ (Sigma, St. Louis, MO, C-3881), 0.3 mM $MgSO_4{\cdot}7H_2O$ (Sigma, 230391), 0.43 mM K_2HPO_4 (Sigma P 3786), 1.29 mM KH_2PO_4 (Sigma P 0662), 0.43 mM NaCl (Fisher S271-500). The pH of the medium was adjusted to 6.8 using 1 M HCl or 1 M NaOH solution.

C. vulgaris is a widely used microalgae for laboratory studies. The autosporangium of *C. vulgaris* can generate 2, 3, 4, 8, 16, or 32 daughter cells (Yamamoto et al., 2003, 2004). Therefore, we anticipate that the growth kinetics of single cells will exhibit distinguishable heterogeneity. Also, we were interested in finding correlation between the size distributions of cells at different stages of growth. Therefore, we studied cells with different sizes suitable for measuring under the microscope. The size of the *C. vulgaris* studied was ~3 to 11 µm.

Determining the Algae Growth Kinetics and Cell Size Distribution in Microfluidic Drops

To observe growth kinetics, the microdevice was kept in a 8- and 16-h cycles of dark and light, respectively. The intensity of the light was 905 lux. The humidity and the temperature of the laboratory where experiments were conducted were 60% and 21°C, respectively. Since the

growth medium was supplied with glucose, we did not introduce any additional CO_2. The CO_2 can diffuse through the PDMS membrane (Webb and Teja, 1999), therefore, it was assumed that the droplets were in equilibrium with the atmospheric CO_2. The same was assumed for oxygen. Oxygen is produced in the respiration system of the algae. We assumed that the produced oxygen diffused out of the droplets, and the oxygen concentration was in equilibrium with the atmosphere.

To quantify the kinetic parameters, the total number of cells in the droplets was monitored over time until we observed the stationary growth phase. Live or dead cells were not distinguished in our counting. The cells were counted manually once in every day using an inverted microscope with 10×1.6 magnification. The specific growth rate was calculated using the following equation:

$$\mu = \frac{\mathrm{dln}(N)}{\mathrm{d}t} \tag{1}$$

where μ is the specific growth rate, N is the number of cells, and t is the time.

To study cell size distribution at different stages of the growth, *C. vulgaris* was grown in droplets following the same procedure used for single-cell growth kinetics study. In this case, the initial number of cells was high, more than 14, to ensure that the measured properties are statistically significant. Microscopic images of the droplets were taken with 10×1.6 magnification, 2.17 pixel/μm. The cell size (maximum diameter) was measured using the "Image-J" software (www.nih.gov). To check the statistical significance of the difference in the average cell sizes, two-tailed paired *t*-test was used.

Results and Discussion

Statistics of Algal Cell Encapsulation in Microfluidic Drop Arrays

To encapsulate an intended number of cells, first we developed a correlation between the number of cells per milliliter of the feed culture and the number of cells captured in each of the droplet. To find the correlation, we used four different feed cultures with 6.2, 4.0, 1.8, and 1.5×10^5 cells/mL, as measured using hemacytometer. After creating droplets, the cell numbers trapped in the droplets were counted under the microscope manually. Since the cell encapsulation in each droplet was independent, it was expected that the cell-trapping will follow Poisson distribution. We checked Poisson statistics of cell encapsulation using the following equation:

$$f(n,\lambda) = \frac{\lambda^n \mathrm{e}^{-\lambda}}{n!} \tag{2}$$

where, f is the probability of encapsulating n is the number of cells in the droplets, and λ is the average number of cells in the droplets.

The use of hydrostatic pressure in droplet trapping showed that a linear correlation exists between the number of cells encapsulated in the droplets and the number of cells per milliliter in the feed culture (Fig. 4A). The trend line in the Figure 4A shows a negative intercept when number of cells per milliliter of the feed is below 1×10^5 which indicates that the cell encapsulation will not hold the linear relation when very dilute culture is used as the feed. The results of Figure 4A were used as a guideline to trap different number of cells. To capture a single cell we used seed culture with 1.3×10^5 cell/mL.

Cell encapsulation followed Poisson distribution as shown in Figure 4B. Therefore, when we tried to encapsulate single cells, many droplets were empty and some of the droplets trapped more than one cell. The Poisson distribution plot combined with Figure 4A gave us an estimated number of droplets that could encapsulate single or multiple cells. The apparent deviation of the experimental and theoretical value in Figure 4B was due to small number of droplets. In our chip there were 30 droplets. The deviation could be reduced if the number of droplets were increased. Figure 4C shows drops capturing 1, 2, 3, and 4 cells.

Long-Term Storage of Droplets in PDMS Chip

In our initial attempts, we made microfluidic devices bonded to glass slide, and we observed drops to shrink to 5% of its original volume within 2 days (Fig. 5A). Due to the shrinkage of the droplets, cells were compressed to a tiny area in the mineral oil and it was not possible see any growth, as shown in Figure 5B. When the storage set-up was modified to that described in Figure 3, the droplets could be stored for extended periods of time as shown in Figure 5. In our experiments, the droplets were stored from 10 to 33 days. To our knowledge, this prolonged storage of nanoliter-scale drops up to a month in PDMS devices has not been demonstrated before in the literature. Maintaining the volume of the droplets was important because the change of volume would alter the concentration of the salts and the substrate inside the droplets. Such concentration variations would make it difficult to compare the growth kinetics between droplets. Since the PDMS membrane is permeable to water but not to the salts, maintaining the volume makes sure that the salts and substrate concentrations remain same (Shim et al., 2007). Using our storage technique, we were able to maintain the volume of the droplets within +4.4% to −11.5% of their original sizes. As shown in Figure 5A, the droplets were shrunk by 11.5% on average on day 8 and swelled by 4.4% on average on day 24. This fluctuation in drop volume is possibly due to slight variations in room temperature, and humidity.

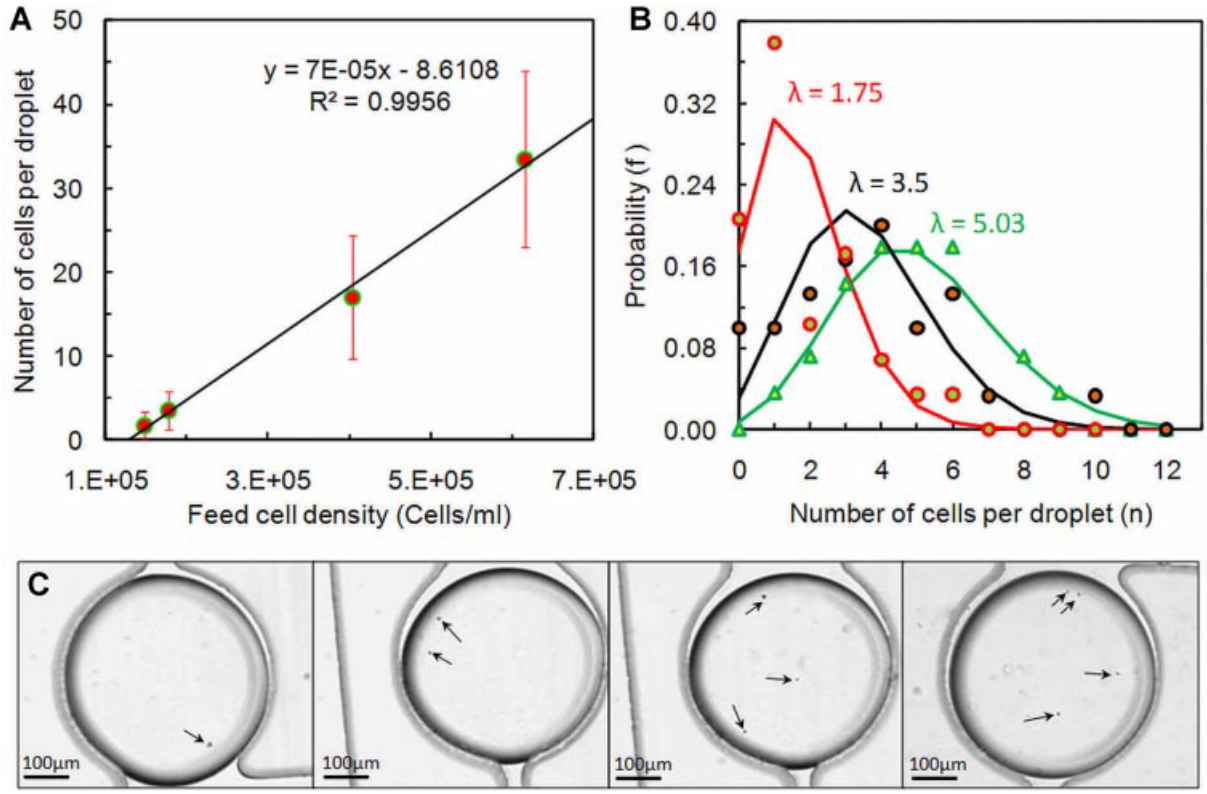

Figure 4. Statistics of algal cell encapsulation in the droplets. **A**: Relation between the average number of cells trapped inside the droplets with the number of cells per milliliter in the feed. **B**: The cell encapsulation followed Poisson distribution. Solid line is probability calculated using Poisson distribution equation, symbols are experimental data, and λ is the average number of cells in the droplets. **C**: Images showing encapsulation of different number of cells in microfluidic drops. Each arrow indicates a trapped algae cell.

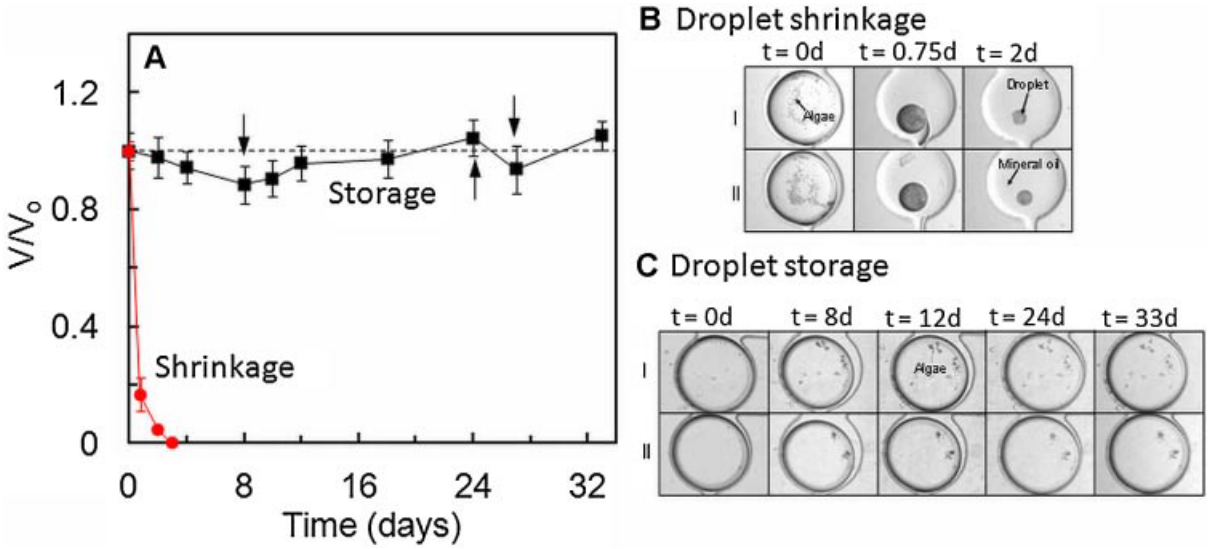

Figure 5. **A**: Change of volume of the droplets (V) with respect to initial volume (V_0) in droplet shrinkage (i.e., devices bonded to glass slide) and long-term storage (i.e., devices bonded to PDMS membrane). The arrow indicates the time when the aperture of the cover slip was increased (upward arrow) or decreased (downward arrow). **B**: Example of shrinkage of two droplets in a PDMS chip mounted on a glass slide, without water reservoir underneath the device. **C**: Example of long-term storage of two droplets in a PDMS chip with thin membrane at the bottom, and water reservoir underneath.

Heterogeneous Growth of Single-Cell *C. vulgaris*

Figure 6A shows growth curves of single cells in five different droplets, all of which were trapped in the same chip. Figure 6B shows microscopy images of the same droplet at different stages of growth for the curve 4 in Figure 6A. The table beside Figure 6A shows the final cell numbers in different droplets; cell numbers varied from 13 to 81. Although all the cells came from the same seed culture and grown in identical conditions in the droplets of the same microfluidic chip, the final cell numbers were significantly different. The specific growth rate determined from the exponential growth phase ranged from 0.55 to 1.52 day^{-1}. We observed similar heterogeneous growth for single cells in repeated experiments.

Cell division of *C. vulgaris* does not follow simple cell doubling hypothesis. Instead, different cell may divide at different rates. This is probably one of the reasons for observing the heterogeneity in single-cell growth. As shown by Yamamoto et al., a single *C. vulgaris* cell may produce 2, 3, 4, 5, 16, and 32 daughter cells (Yamamoto et al., 2003, 2004). We also have found that in microfluidic drops, a single *C. vulgaris* cell to produce 3, 4, and 5 daughter cells. Figure 6C shows example of division of *C. vulgaris*. These are snap shots of cells showing partition of chloroplast (Fig. 6C(I, II, IV)). The partitioned chloroplast will later be encapsulated into daughter cells after completion of the cell division process. Another cause of the heterogeneity could be that each encapsulated single cell is at a different stage of its life cycle.

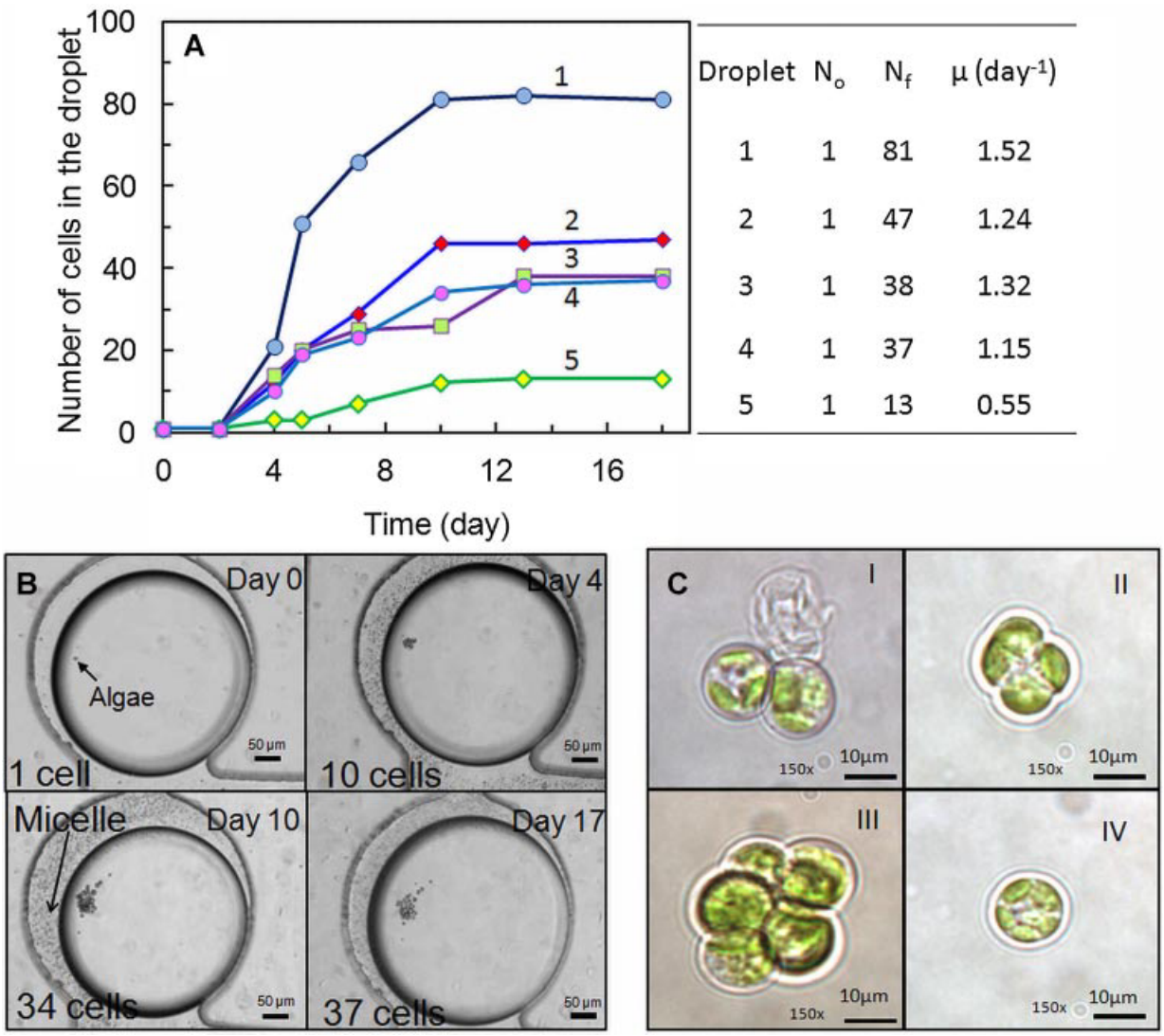

Figure 6. **A**: Single cell growth kinetics; the table beside shows the initial cell number (N_0), final cell number (N_f), and the specific growth rate (μ). **B**: Microscopy images of the droplet for the curve 4 in (A) at different stages of the growth. The dark spots outside the droplets are surfactant micelles. The surfactant formed the micelle when the water diffused to the mineral oil. **C**: Light microscopy image of *C. vulgaris* cell division.

To assess the differences in single-cell growth kinetics with bulk-scale growth, we compared the growth kinetics of multiple cells in same microfluidic droplets, and in bulk scale experiments in a 1 L bioreactor. Figure 7A shows an example of growth kinetics of multiple cells observed in microfluidic droplets. In this case, all three droplets were started with same number of cells ($N_0 = 14$). The growth curves overlaps with relatively small variations and the final cell numbers become 371 and 383, and 335. Figure 7B shows variation of the final cell number (N_f) with respect to initial cell number (N_0) in various droplets after 15 days. It shows that single-cell has higher cellular yield (final to initial cell number) and the heterogeneity of growth kinetics is less prominent in the case of multiple cells. The heterogeneity is less prominent, compared to single cells, because of the statistical averaging of multiple cells. Figure 7C shows the result of bulk scale experiments. The cell density is shown as the number of cells per 10 nL because the average volume of the droplets in the microfluidic experiment is ~10 nL. The specific growth rate calculated from this bulk scale experiment was 1.12 day^{-1} which is close to the average value (1.16 day^{-1}) of the specific growth rates of single cells determined from the five droplets shown on the table beside Figure 6A. However, the number of cells per unit volume is much higher in the droplets than that in the bulk (Fig. 7A and 7C).

Variation in Cell Size at Different Stages of *C. vulgaris* Growth

Figure 8A shows the changes in average cell size at different stages of growth of *C. vulgaris* inside microfluidic droplets. Both the growth and cell size were measured from three different experiments starting with same number of cells in the droplets. The average cell size increases during the lag phase and stationary growth phases but decreases at exponential growth phase. The decrease of cell size during exponential phase was due to smaller cells being reproduced during cell division. Similar result was observed by Griffiths (1963). In a bulk scale experiment, Griffiths monitored size distribution of *C. vulgaris* by measuring the mean diameter of the cells observed in the hemocytometer slide. They used a calibrated micrometer eye-piece to measure the size and a minimum of 50 cells were measured in each case. They found that average cell size increased during the lag phase and then decreased slightly during the exponential phase. They did not measure the cell size during the stationary phase (Griffiths, 1963). In our study, the average cell size changed from 5.99 μm (SD: 1.08) to 7.33 μm (SD: 1.3) from exponential to stationary growth phase. The smallest and the largest cells were 2.3 and 12.6 μm, respectively.

Figure 8B shows an example of size distribution of the entire cell population at different stages of growth in a droplet for the growth curve shown in the same plot. The size distribution is bell-shaped and shifted towards the right due to increase of cell sizes. The statistical analysis of this

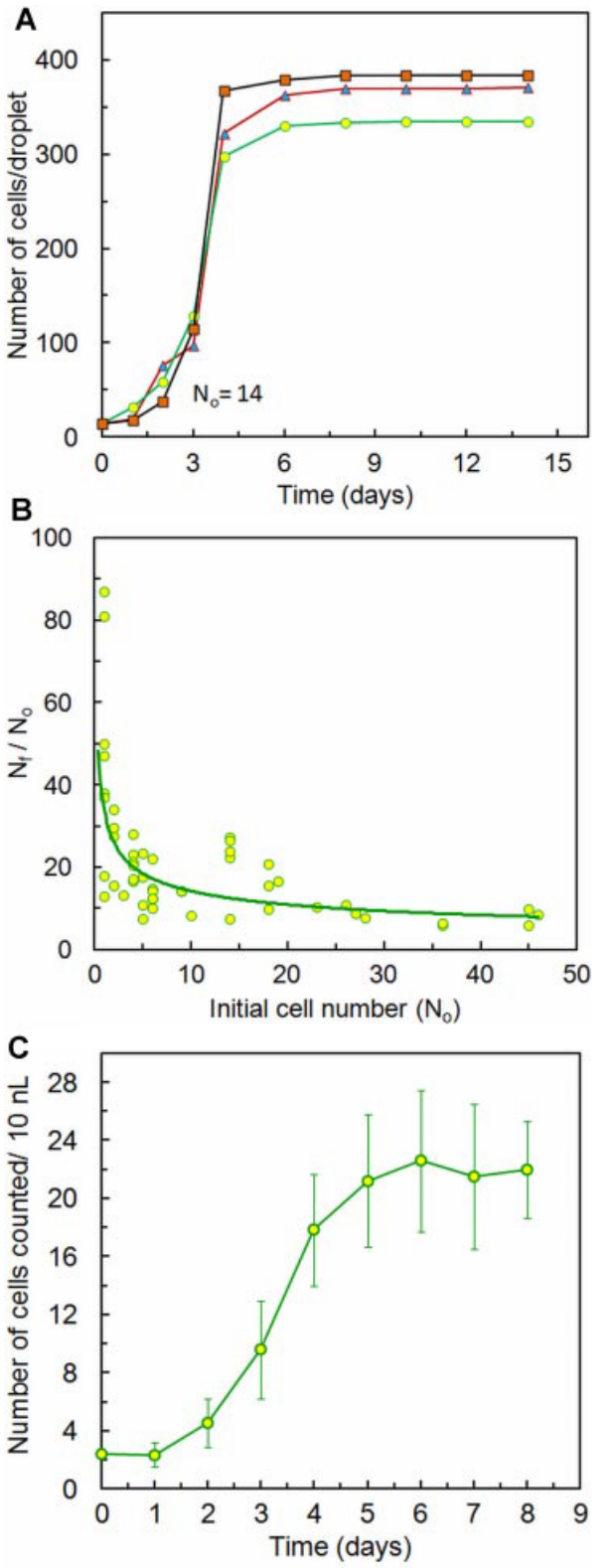

Figure 7. **A**: Growth curves observed in three droplets with initial cell number, $N_0 = 14$. **B**: Ratio of final cell number (N_f) to the initial cell number (N_0) observed in various microfluidic experiments. **C**: Growth curve of *Chlorella vulgaris* in bulk scale experiment in 1 L bioreactor. To compare the results with microfluidic experiments, the number of cells was recalculated for 10 nL which is the average volume of the droplets.

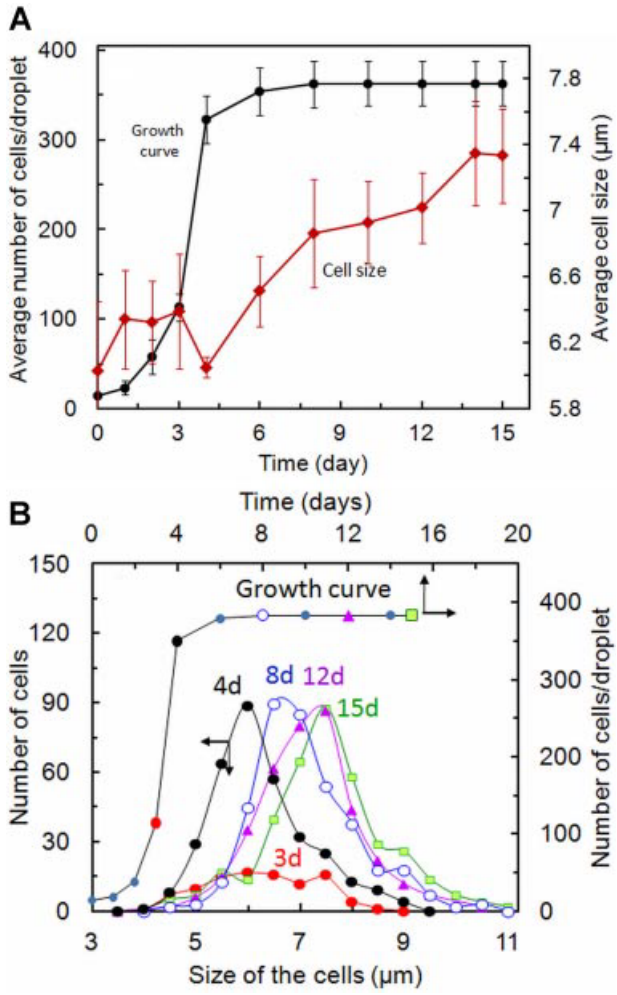

Figure 8. Changes in cell size at different stages of the growth. **A**: Growth curve and average cell sizes at different stages of the growth. The values are averaged from three different experiments. The bars are standard deviation between experiments. **B**: Example size distribution of the cells observed in a droplet at different days. Similar size distribution was observed in replicate experiments.

distribution using two-tailed paired *t*-test shows that the *P*-values are 0.0001, 0.0001, and 0.013 with 95% confidence interval when the cell sizes are compared between 15 and 12, 12 and 4, and 4 and 3 days, respectively. For the same test, the *P*-value was 0.9767 when the size distribution was compared for day 14 and 15. These *P*-values indicate that the increase in average cell size is statistically significant at stationary growth phase from days 4 to 14. The change was not significant from days 14 to 15. We did not observe any further change after day 15. Although we find that changes in cell size at stationary phase are statistically significant, the reason for this change is not precisely known. It is possible that the cells produce more fatty acids during the stationary phase. In other word, the older cells may accumulate more fatty acids than the younger cells. If that is true, this result will have an impact in the area of biofuels production from algae. However, this is still a hypothesis that remains to be examined.

Conclusions

Aqueous droplets can be stored in PDMS microfluidic chip as long as needed. We stored droplets for 33 days. Droplet-microfluidic chip can be used to study growth kinetics of single or multiple algae cells. Growth kinetics of single-cell *C. vulgaris* shows significant heterogeneity compared to that observed in larger number of cells and bulk scale experiments. Cell size changes significantly at different stages of cell growth. The mean cell size increases in lag and stationary phase and decreases in exponential phase. The developed technique of storing droplets and growing algae cell can be used for rapid screening of growth conditions if the droplets are generated with well-defined variation of growth conditions from drop-to-drop (Sun et al., 2011). The results of this study will have impact in the area of algal oil harvesting if the change of cell size is related to oil content.

We thank Swastika S. Bithi for fabricating the molds used in this study. M.N. Karim thanks AT & T Foundation, Texas Tech University for the funding for this research. S. A. Vanapalli acknowledges partial support from Agriculture and Food Research Initiative Grant 2009-02400 from the USDA National Institute of Food and Agriculture and the Texas Tech University Honors College.

References

Bithi SS, Vanapalli SA. 2010. Behavior of a train of droplets in a fluidic network with hydrodynamic traps. Biomicrofluidics 4(4):044110(1)–044110(10).

Boukellal H, Selimovic S, Jia YW, Cristobal G, Fraden S. 2009. Simple, robust storage of drops and fluids in a microfluidic device. Lab Chip 9(2):331–338.

Brouzes E, Medkova M, Savenelli N, Marran D, Twardowski M, Hutchison JB, Rothberg JM, Link DR, Perrimon N, Samuels ML. 2009. Droplet microfluidic technology for single-cell high-throughput screening. Proc Natl Acad Sci USA 106(34):14195–14200.

Chen CY, Yeh KL, Su HM, Lo YC, Chen WM, Chang JS. 2010. Strategies to enhance cell growth and achieve high-level oil production of a *Chlorella vulgaris* isolate. Biotechnol Progr 26(3):679–686.

Collier JL. 2000. Flow cytometry and the single cell in phycology. J Phycol 36(4):628–644.

Doyle PS, Randall GC. 2005. Permeation-driven flow in poly(dimethylsiloxane) microfluidic devices. Proc Natl Acad Sci USA 102(31):10813–10818.

Falconnet D, Niemisto A, Taylor RJ, Ricicova M, Galitski T, Shmulevich I, Hansen CL. 2011. High-throughput tracking of single yeast cells in a microfluidic imaging matrix. Lab Chip 11(3):466–473.

Griffiths DJ. 1963. The effect of glucose on cell division in *Chlorella vulgaris*, beijerinck (emerson strain). Ann Bot 27(8):493–504.

Huebner A, Srisa-Art M, Holt D, Abell C, Hollfelder F, deMello AJ, Edel JB. 2007. Quantitative detection of protein expression in single cells using droplet microfluidics. Chem Commun (12): 1218–1220. DOI: 10.1039/B618570C

Koch AL, Robertson BR, Button DK. 1996. Deduction of the cell volume and mass from forward scatter intensity of bacteria analyzed by flow cytometry. J Microbiol Methods 27(1):49–61.

Kortmann H, Blank LM, Schmid A. 2009. Single cell analysis reveals unexpected growth phenotype of *S. cerevisiae*. Cytometry, Part A 75A(2):130–139.

Koster S, Angile FE, Duan H, Agresti JJ, Wintner A, Schmitz C, Rowat AC, Merten CA, Pisignano D, Griffiths AD, Weitz DA. 2008. Drop-based microfluidic devices for encapsulation of single cells. Lab Chip 8(7): 1110–1115.

Lee PJ, Hung PJ, Rao VM, Lee LP. 2006. Nanoliter scale microbioreactor array for quantitative cell biology. Biotechnol Bioeng 94(1):5–14.

Liang YN, Sarkany N, Cui Y. 2009. Biomass and lipid productivities of *Chlorella vulgaris* under autotrophic, heterotrophic and mixotrophic growth conditions. Biotechnol Lett 31(7):1043–1049.

Lindström S. 2009. Microwell devices for single-cell analyses. Stockholm. Royal Institute of Technology: 92 p.

Marcoux PR, Dupoy M, Mathey R, Novelli-Rousseau A, Heran V, Morales S, Rivera F, Joly PL, Moy JP, Mallard F. 2011. Micro-confinement of bacteria into w/o emulsion droplets for rapid detection and enumeration. Colloids Surf, A 377(1–3):54–62.

Onoe H, Takeuchi S. 2008. Microfabricated mobile microplates for handling single adherent cells. J Micromech Microeng 18(9):095003(1)–095003(7).

Pan J, Stephenson AL, Kazamia E, Huck WTS, Dennis JS, Smith AG, Abell C. 2011. Quantitative tracking of the growth of individual algal cells in microdroplet compartments. Integr Biol 3(10):1043–1051.

Powell EE, Mapiour ML, Evitts RW, Hill GA. 2009. Growth kinetics of *Chlorella vulgaris* and its use as a cathodic half cell. Bioresour Technol 100(1):269–274.

Rittmann BE. 2008. Opportunities for renewable bioenergy using microorganisms. Biotechnol Bioeng 100(2):203–212.

Rodolfi L, Chini Zittelli G, Bassi N, Padovani G, Biondi N, Bonini G, Tredici MR. 2009. Microalgae for oil: Strain selection, induction of lipid synthesis and outdoor mass cultivation in a low-cost photobioreactor. Biotechnol Bioeng 102(1):100–112.

Schmitz CHJ, Rowat AC, Koster S, Weitz DA. 2009. Dropspots: a picoliter array in a microfluidic device. Lab Chip 9(1):44–49.

Shim JU, Cristobal G, Link DR, Thorsen T, Jia YW, Piattelli K, Fraden S. 2007. Control and measurement of the phase behavior of aqueous solutions using microfluidics. J Am Chem Soc 129(28):8825–8835.

Shim JU, Olguin LF, Whyte G, Scott D, Babtie A, Abell C, Huck WTS, Hollfelder F. 2009. Simultaneous determination of gene expression and enzymatic activity in individual bacterial cells in microdroplet compartments. J Am Chem Soc 131(42):15251–15256.

Sun M, Bithi SS, Vanapalli SA. 2011. Microfluidic static droplet arrays with tuneable gradients in material composition. Lab Chip 11:3949–3952.

Tang H, Chen M, Garcia MED, Abunasser N, Ng KYS, Salley SO. 2011. Culture of microalgae *Chlorella minutissima* for biodiesel feedstock production. Biotechnol Bioeng 108(10):2280–2287.

Trivedi V, Doshi A, Kurup GK, Ereifej E, Vandevord PJ, Basu AS. 2010. A modular approach for the generation, storage, mixing, and detection of droplet libraries for high throughput screening. Lab Chip 10(18): 2433–2442.

Um E, Lee SG, Park JK. 2010. Random breakup of microdroplets for single-cell encapsulation. Appl Phys Lett 97(15):153703(1)–153703(3).

Webb KF, Teja AS. 1999. Solubility and diffusion of carbon dioxide in polymers. Fluid Phase Equilib 160:1029–1034.

Weyer KM, Bush DR, Darzins A, Willson BD. 2010. Theoretical maximum algal oil production. Bioenergy Res 3(2):204–213.

Wu HW, Volponi JV, Oliver AE, Parikh AN, Simmons BA, Singh S. 2011. In vivo lipidomics using single-cell Raman spectroscopy. Proc Natl Acad Sci USA 108(9):3809–3814.

Yamamoto M, Nozaki H, Miyazawa Y, Koide T, Kawano S. 2003. Relationship between presence of a mother cell wall and speciation in the unicellular microalga *Nannochloris* (*Chlorophyta*). J Phycol 39(1):172–184.

Yamamoto M, Fujishita M, Hirata A, Kawano S. 2004. Regeneration and maturation of daughter cell walls in the autospore-forming green alga *Chlorella vulgaris* (*Chlorophyta*, *Trebouxiophyceae*). J Plant Res 117(4): 257–264.